A Finite Volume Meshless Local Petrov-Galerkin Method for Topology Optimization Design of the Continuum Structures

Juan Zheng[1,2,3]**, Shuyao Long**[1,2]**, Yuanbo Xiong**[1,2] **and Guangyao Li**[1]

Abstract: In this paper, the finite volume meshless local Petrov-Galerkin method (FVMLPG) is applied to carry out a topology optimization design for the continuum structures. In FVMLPG method, the finite volume method is combined with the meshless local Petrov-Galekin method, and both strains as well as displacements are independently interpolated, at randomly distributed points in a local domain, using the moving least squares (MLS) approximation. The nodal values of strains are expressed in terms of the independently interpolated nodal values of displacements, by simple enforcing the strain-displacement relationships directly. Considering the relative density of nodes as design variable, and the minimization of compliance as objective function, the mathematical formulation of the topology optimization design is developed using the solid isotropic microstructures with penalization (SIMP) interpolation scheme. The topology optimization problem is solved by the optimality criteria method. Numerical examples show that the proposed approach is feasible and efficient for the topology optimization design of the continuum structures.

Keywords: finite volume meshless local Petrov-Galerkin method (FVMLPG); moving least squares (MLS); topology optimization design for continuum structures; SIMP; optimality criteria method

1   Introduction

The topology optimization design of the continuum structures is one of the most challenging research topics in the field of the structural optimization [Bendsoe and Sigmund (2003)]. The purpose of the topology optimization design is to find the

---

[1] State Key Laboratory of Advanced Design and Manufacture for Vehicle Body, Hunan University, Changsha, China

[2] College of Mechanics and Aerospace Engineering, Hunan University, Changsha, China

[3] Corresponding author. Tel.: +86-0731-8824724. E-mail: dingdang8209@163.com

optimal lay-out of a structure within a specified region. In this problem the only known quantities are the applied loads, the possible support conditions, the volume of the structure to be constructed and possibly some additional design restrictions, and the physical size and the shape of the structure are unknown. The topology optimization design of the continuum structures is essentially a discretized 0-1 variables problem. Recently, with the increase of interest in this field, various models and methods for structural topology optimization were explored, with goals of improving the computational efficiency, and alleviating numerical instabilities [Cisilino (2006), Li and Atluri (2008a,b), Michael and Wang (2004), Michael and Zhou (2004), Tapp, Hansel, Mittelstedt and Becker (2004), Wang and Wang (2006), Wang, Lim, Khoo and Wang (2007a, b, c, 2008), Zheng, Long, Xiong and Li (2008), Zhou and Wang (2006)]. For the topology optimization design of the continuum structures, homogenization approach [Bendsoe and Kikuchi (1988)], variable density approach [Bendsoe and Sigmund (1999)] and evolutionary structural optimization (ESO) approach [Zhou and Rozvany (2001)] are often employed. In the variable density approach, a density function $\rho(x)$, which varies from zero (void state) to unity (solid state), is introduced to represent the material distribution in the design domain. Solid isotropic microstructures with penalization (SIMP) [Bendsoe and Sigmund (1999)] and rational approximation of material properties (RAMP) [Stolpe and Svanberg (2001)] are two common density interpolation models.

To date, the numerical method prevailing in topology optimization design is the finite element method (FEM). However, FEM has a big limitation continuously remeshing the finite element model when dealing with large deformation or moving boundary problems. Meshless methods have been achieved remarkable progress in recent years, mainly due to the possibility of overcoming the drawbacks of mesh-based method, such as the labor-intensive process of mesh-generation, locking, etc. The meshless methods may also eliminate the mesh distortion problems once the solid/structure undergoes large deformations. Several meshless methods have been developed, based on global weak forms, such as smooth particle hydrodynamics (SPH) [Monaghan (1992)], and element-free Galekin method (EFG) [Belytschko and Lu et al. (1994)] and so on. They require certain meshes or background cells over the solution domain, for purposes of integration of the weak form, which may also become distorted during large deformations. In contrast, the meshless local Petrov-Galerkin (MLPG) method [Atluri and Zhu (1998), Atluri and Shen (2002), Chen, Liu and Cen (2008)] is based on writing the local weak forms of PDES, over overlapping local sub-domains. The integration of the weak form is also performed within the local sub-domains, thus negating any need for any kind of meshes and background cells, making the MLPG approaches a truly meshless

method. More recently, a new meshless mixed finite volume method has been presented by [Atluri, Han and Rajendran (2004)]. The mixed method has been applied to solve the elasto-static problems [Atluri, Han and Rajendran (2004)] and the non-linear problems with large deformations and rotations [Han, Rajendran and Atluri (2005)].

In this paper, the topology optimization design for the continuum structures is formulated using finite volume meshless local Petrov-Galerkin method for two-dimensional elastostatics problems. In FVMLPG, the finite volume method is combined with the meshless local Petrov-Galekin method. Starting from an integral form of the governing equations over a local sub-domain, both strains as well as displacements are independently interpolated, at randomly distributed points in a local domain, using the MLS approximation. The nodal values of strains are expressed in terms of the independently interpolated nodal values of displacements, by simple enforcing the strain-displacement relationships directly. And a direct interpolation method is used to impose the essential boundary conditions [Liu and Yan (2000)]. Considering the relative density of nodes as design variable, and the minimization of compliance as objective function, the mathematical formulation of the topology optimization design is developed using the SIMP interpolation scheme. The topology optimization problem is solved by the optimality criteria method. Finally, the feasibility and efficiency of the proposed method are illustrated with several 2D examples that are widely used in the topology optimization design.

2 Moving least square approximation

The moving least square (MLS) method is generally considered to be one of the best schemes to interpolate data with reasonable accuracy. If field variable is a function such as $u(\mathbf{x})$, the interpolation function $u^h(\mathbf{x})$ in a sub-domain Ω_s can be defined over a number of scattered local points $x_i(i = 1, 2, \ldots, n)$ by

$$u^h(\mathbf{x}) = \mathbf{P}^{\mathrm{T}}(\mathbf{x})\mathbf{a}(\mathbf{x}), \ \forall \mathbf{x} \in \Omega_s \tag{1}$$

where $\mathbf{P}^{\mathrm{T}}(\mathbf{x})$ is a complete monomial basis function of order m. For two-dimensional problems, the complete monomial basis function are chosen as

linear basis function $\mathbf{P}^{\mathrm{T}}(\mathbf{x}) = [1, x_1, x_2]$, m=3

quadratic basis function $\mathbf{P}^{\mathrm{T}}(\mathbf{x}) = \left[1, x_1, x_2, x_1^2, x_1 x_2, x_2^2\right]$, m=6

and $\mathbf{a}(\mathbf{x})$ is a vector containing coefficients which are functions of the global Cartersian coordinates $[x_1, x_2]^{\mathrm{T}}$, depending on the monomial basis.

These coefficients can be obtained by minimizing a weighted discrete $\mathbf{L}_2$ norm defined as

$$J(x) = \sum_{i=1}^{n} w(\mathbf{x}_i, \mathbf{x})[\mathbf{P}^{\mathrm{T}}(\mathbf{x}_i)\mathbf{a}(\mathbf{x}) - \hat{u}_i]^2 \tag{2}$$

where n is the number of nodes in the support domain of $\mathbf{x}$ for which the weight function $w(\mathbf{x}_i, \mathbf{x}) > 0$; u_i is the nodal parameter of u at $\mathbf{x} = \mathbf{x}_i$; and $w(\mathbf{x}_i, \mathbf{x})$ is the weight function associated with the node i. In this paper, weight function is cubic spline weight function as below

$$w(\mathbf{x}_i, \mathbf{x}) = \begin{cases} 2/3 - 4r_i^2 + 4r_i^3 & r_i \leq 0.5 \\ 4/3 - 4r_i + 4r_i^2 - 4/3r_i^3 & 0.5 < r_i \leq 1 \\ 0 & r_i > 1 \end{cases}$$

where $r_i = \frac{d_i}{r_w} = \frac{|\mathbf{x}-\mathbf{x}_i|}{r_w}$, in which $d_i = |\mathbf{x} - \mathbf{x}_i|$ is the distance from node $\mathbf{x}_i$ to the interest point $\mathbf{x}$, and r_w is the size of the support domain for the weight function.

The stationary of J with respect to $\mathbf{a}(\mathbf{x})$ leads to the following set of linear relation

$$\mathbf{A}(\mathbf{x})\mathbf{a}(\mathbf{x}) = \mathbf{B}(\mathbf{x})\mathbf{U}_s \tag{3}$$

where $\mathbf{U}_s$ is the vector that collects the nodal parameters of the field function for all the nodes in the support domain, $\mathbf{U}_s = [\hat{u}_1, \hat{u}_2, \ldots, \hat{u}_n]^{\mathrm{T}}$; and $\mathbf{A}(\mathbf{x})$ is called the weighted moment matrix defined by

$$\mathbf{A}(\mathbf{x}) = \mathrm{P}^{\mathrm{T}}\mathrm{W}\mathrm{P} = \sum_{i=1}^{n} w(\mathbf{x}_i, \mathbf{x})\mathbf{P}(\mathbf{x}_i)\mathbf{P}^{\mathrm{T}}(\mathbf{x}_i)$$

the matrix $\mathbf{B}$ in Equation (3) is defined as

$$\mathbf{B}(\mathbf{x}) = \mathrm{P}^{\mathrm{T}}\mathbf{W} = [w(\mathbf{x}_1, \mathbf{x})\mathbf{P}(\mathbf{x}_1), w(\mathbf{x}_2, \mathbf{x})\mathbf{P}(\mathbf{x}_2), \ldots, w(\mathbf{x}_n, \mathbf{x})\mathbf{P}(\mathbf{x}_n)]$$

Solving Equation (3) for $\mathbf{a}(\mathbf{x})$, we have

$$\mathbf{a}(\mathbf{x}) = \mathbf{A}^{-1}(\mathbf{x})\mathbf{B}(\mathbf{x})\mathbf{U}_s$$

Substituting the above equation back into Equation (1), we have

$$u^h(\mathbf{x}) = \sum_{i=1}^{n} \phi_i(\mathbf{x})\hat{u}_i = \mathbf{\Phi}^{\mathrm{T}}(\mathbf{x})\mathbf{U}_s \tag{4}$$

where $\mathbf{\Phi}(\mathbf{x})$ is the vector of MLS shape functions corresponding n nodes in the support domain of the point $\mathbf{x}$, and can be written as

$$\mathbf{\Phi}^{\mathrm{T}}(\mathbf{x}) = [\phi_1(\mathbf{x})\phi_2(\mathbf{x})\ldots\phi_n(\mathbf{x})] = \mathbf{P}^{\mathrm{T}}(\mathbf{x})\mathbf{A}^{-1}(\mathbf{x})\mathbf{B}(\mathbf{x}) \tag{5}$$

3 Finite volume meshless local Petrov-Galerkin method (FVMLPG)

Consider the following standard two-dimension problem of linear elasticity defined in the domain Ω bounded by the boundary Γ

$$\begin{cases} \sigma_{ij,j} + b_i = 0, & \text{in } \Omega \\ u_i = \bar{u}_i, & \text{on } \Gamma_u \\ t_i = \sigma_{ij} n_j = \bar{t}_i, & \text{on } \Gamma_t \end{cases} \tag{6}$$

where σ_{ij} is the stress tensor, which corresponds to the displacement field u_i; b_i is a body force vector; $\bar{t}_i$ is the prescribed traction on the natural boundaries; $\bar{u}_i$ is the prescribed displacement on the essential boundaries; n_j is the vector of unit outward at a point on the natural boundary.

The FVMLPG method establishes equations node by node, which makes it possible to use different sets of equations for the different nodes. In this paper, we use two different sets of equations for the essential boundary nodes and not essential boundary nodes, respectively.

For node **x** not located on the essential boundary, we start from an integral form over a local sub-domain Ω_s and use the MLS approximation to develop the FVMLPG method. The integral form of Equation (1) over the sub-domain Ω_s can be written as follows

$$\int_{\Omega_s} (\sigma_{ij,j} + b_i) \mathrm{d}\Omega = 0 \tag{7}$$

Applying the divergence theorem to the first integral term leads to

$$\int_{\Gamma_s} \sigma_{ij} n_j \mathrm{d}\Gamma + \int_{\Omega_s} b_i \mathrm{d}\Omega = 0 \tag{8}$$

The boundary Γ_s for the local quadrature domain Ω_s has composed by two parts, i.e., $\Gamma_s = \Gamma_{si} \cup \Gamma_{st}$, where
Γ_{si} is the internal boundary of the quadrature domain, which does not intersect with the global boundary Γ;
Γ_{st} is the part of the natural boundary that intersects with the quadrature domain;

By considering the traction boundary conditions and imposing it in Equation (8) leads to

$$\int_{\Gamma_{si}} t_i \mathrm{d}\Gamma + \int_{\Gamma_{st}} \bar{t}_i \mathrm{d}\Gamma + \int_{\Omega_s} b_i \mathrm{d}\Omega = 0 \tag{9}$$

For simplicity, Equation (9) can be written in matrix form as

$$\int_{\Gamma_{si}} \mathbf{t} \mathrm{d}\Gamma = -\int_{\Gamma_{st}} \bar{\mathbf{t}} \mathrm{d}\Gamma - \int_{\Omega_s} \mathbf{b} \mathrm{d}\Omega \tag{10}$$

With the constitutive relations of an isotropic linear elastic homogeneous solid, the tractions in Equation (9) can be written in term of the strains, as

$$t_i = \sigma_{ij} n_j = D_{ijkl} \varepsilon_{kl} n_j \tag{11}$$

The strains can be independently interpolated with the shape function, as

$$\varepsilon_{kl} = \sum_{i=1}^{np} \phi^{(i)} \hat{\varepsilon}_{kl}^{(i)} \tag{12}$$

Substituting Equation (12) to Equation (11), and written in matrix form, we can have

$$\mathbf{t} = \mathbf{nDT}\hat{\boldsymbol{\varepsilon}} \tag{13}$$

where

$$\mathbf{t} = \begin{Bmatrix} t_1 \\ t_2 \end{Bmatrix}, \quad \mathbf{n} = \begin{bmatrix} n_x & 0 & n_y \\ 0 & n_y & n_x \end{bmatrix}, \quad \mathbf{D} = \frac{E}{1-\mu^2} \begin{bmatrix} 1 & \mu & 0 \\ \mu & 1 & 0 \\ 0 & 0 & (1-\mu)/2 \end{bmatrix},$$

$$\mathbf{T} = \{\mathbf{T}_1, \quad \mathbf{T}_2, \quad \cdots, \quad \mathbf{T}_n\}^{\mathrm{T}}, \quad \hat{\boldsymbol{\varepsilon}} = \{\hat{\boldsymbol{\varepsilon}}_1, \quad \hat{\boldsymbol{\varepsilon}}_2, \quad \cdots, \quad \hat{\boldsymbol{\varepsilon}}_n\}^{\mathrm{T}}$$

in which

$$\mathbf{T}_i = \begin{bmatrix} \phi_i & 0 & 0 \\ 0 & \phi_i & 0 \\ 0 & 0 & \phi_i \end{bmatrix}, \quad \hat{\boldsymbol{\varepsilon}}_i = \begin{Bmatrix} \hat{\varepsilon}_1^i \\ \hat{\varepsilon}_2^i \\ \hat{\varepsilon}_3^i \end{Bmatrix}$$

At now, by substituting Equation (13), Equation (10) can be written, as

$$\int_{\Gamma_{si}} \mathbf{nDT}\hat{\boldsymbol{\varepsilon}} \mathrm{d}\Gamma = -\int_{\Gamma_{st}} \bar{\mathbf{t}} \mathrm{d}\Gamma - \int_{\Omega_s} \mathbf{b} \mathrm{d}\Omega$$

It can be rewritten as

$$\mathbf{R}\hat{\boldsymbol{\varepsilon}} = \mathbf{F} \tag{14}$$

where

$$\mathbf{R} = \int_{\Gamma_{si}} \mathbf{nDT} \mathrm{d}\Gamma, \quad \mathbf{F} = -\int_{\Gamma_{st}} \bar{\mathbf{t}} \mathrm{d}\Gamma - \int_{\Omega_s} \mathbf{b} \mathrm{d}\Omega$$

The advantage of Equation (14) is that it does not contain any derivatives of the shape function. Instead, in traditional MLPG the equation is written in terms of

the displacement variables, therefore the derivate of the shape function will appear in the discretized local form [Atluri and Shen (2002)]. It is well known that the meshless approximation is not efficient for calculation such derivative everywhere in the domain, especially when the MLS approximation is used. Thus the efficiency of the present method is improved over the traditional MLPG method. On the other hand, the number of equations in Equation (14) is less than the number of the dependent strain variables, because the nodal strain variables are more than the displacement ones. For example, in 2D problem, there are three nodal strain variables, but only two displacement variables. It is possible to reduce the number of variables by transforming the strain variables back to the displacement without charging Equation (14).

For linear elasto-statics, the strain-displacement relations are

$$\boldsymbol{\varepsilon} = \mathbf{Lu} = \begin{bmatrix} \frac{\partial}{\partial x} & 0 \\ 0 & \frac{\partial}{\partial y} \\ \frac{\partial}{\partial y} & \frac{\partial}{\partial x} \end{bmatrix} \begin{Bmatrix} u \\ v \end{Bmatrix} \tag{15}$$

The interpolation of displacement can also be accomplished by using the same shape function, for the nodal displacement variables, as

$$\mathbf{u}^h = \begin{bmatrix} \phi_1 & 0 & \cdots & \phi_n & 0 \\ 0 & \phi_1 & \cdots & 0 & \phi_n \end{bmatrix} \begin{Bmatrix} \hat{u}_1 \\ \hat{v}_1 \\ \vdots \\ \hat{u}_n \\ \hat{v}_n \end{Bmatrix} = \boldsymbol{\Phi}\hat{\mathbf{u}} \tag{16}$$

The two sets of nodal variables can by transformed through a linear algebraic matrix

$$\hat{\boldsymbol{\varepsilon}} = \mathbf{H}\hat{\mathbf{u}} \tag{17}$$

The number of system equations is then reduced to the same number as the nodal displacement variables, after the transformation.

Substituting Equation (17) into (14), the relation between displacement and force is obtained as

$$\mathbf{K}\hat{\mathbf{U}} = \mathbf{F} \tag{18}$$

For node j located on the essential boundary, a direct interpolation method for the imposition of essential boundary conditions is introduced in this paper. This

method was proposed by Liu and Yan [Liu and Yan (2000)]. The direct interpolation method enforces the essential boundary conditions using the equation of MLS approximation

$$u_j^h(\mathbf{x}) = \sum_{i=1}^n \phi_i(\mathbf{x})\hat{u}_i = \bar{u}_j \tag{19}$$

where $\bar{u}_j$ is the specified displacement at node j on the essential boundary.

The Equation (19) is basically a linear algebraic equation for node j on the essential boundary. The essential boundary condition of Equation (19) is directly assembled into the global system equation. This treatment of the essential boundary condition is straightforward and very effective. It simplifies significantly the procedure of imposing essential boundary conditions, and the essential boundary conditions are satisfied exactly. Moreover, computation for all the nodes on the essential boundary has been simplified.

4   Formulation of the topology optimization design

4.1   The SIMP model

SIMP (solid isotropic microstructures with penalization) is a common density interpolation model [Bendsoe and Sigmund (1999)]. In SIMP model, a penalization factor which has the effect of penalizing the intermediate density is introduced to ensure that the continuous design variables are forced towards to a 0-1 solution. The relation between the density and the material tensor is written as

$$E_{ijkl}(x) = \rho^p(x) E_{ijkl}^0 \tag{20}$$

where E_{ijkl}^0 is the Young's modulus of a given solid material, p is a penalization factor.

The density of any point in the design domain can be interpolated by the nodal density parameters and the MLS shape function as follows

$$\rho(x) = \sum_{i=1}^{np} \phi_i \rho_i \tag{21}$$

where ρ_i is the relative density of the ith node, and is the design variable, ϕ_i is the shape function of the ith node; np is the number of nodes in the support domain.

Considering the relative density of the nodes as design variable, and the minimize compliance as objective function, the topology optimization problem based on the

SIMP interpolation scheme can be formulated as follows

$$
\begin{aligned}
&\text{find } \rho\,(x)\,, \ x \in \Omega \\
&\min \quad c = \mathbf{F}^\mathrm{T}\mathbf{U} \\
&\text{s.t.} \quad \mathbf{K}\hat{\mathbf{U}} = \mathbf{F} \\
&\qquad V = \int_\Omega \rho\,(x)\mathrm{d}\Omega = fV_0 \\
&\qquad 0 < \rho_{\min} \le \rho_i \le 1
\end{aligned}
\tag{22}
$$

where $\mathbf{K}$ is the global stiffness matrix; $\mathbf{U}$ is the global displacement vector; $\hat{\mathbf{U}}$ is the parameters of displacements; $\mathbf{F}$ is the global force vector; V is the material volume of the design domain; V_0 is the given volume of the solid material; f is the prescribed volume fraction; $\rho_{\min}$ is a lower bound on density, introduced to prevent any possible singularity, in typical application, we set $\rho_{\min} = 0.001$.

4.2 Solution methods

The topology optimization problem could be solved using several different approaches such as Optimality Criteria (OC) method [Zhou and Rozvany (1991)], Sequential Linear Programming (SLP) method [Fujii and Kikuchi (2000)] or the method of Moving Asymptotes (MMA) [Svanberg (1987)] and others. The OC method is simple to understand and implement, and is computationally efficient. The effectiveness of the method comes from the fact that each design variable is updated independently of the update of the other design variables. Following Sigmund(2001), a updating scheme for the design variables is formulated as follows

$$
\rho_i^{new} = \begin{cases} \max(\rho_{\min},\rho_i - m) & \text{if } \rho_i B_i^\eta \le \max(\rho_{\min},\rho_i - m) \\ \rho_i B_i^\eta & \text{if } \max(\rho_{\min},\rho_i - m) < \rho_i B_i^\eta < \min(1,\rho_i + m) \\ \min(1,\rho_i + m) & \text{if } \min(1,\rho_i + m) \le \rho_i B_i^\eta \end{cases}
\tag{23}
$$

where B_i is given by the expression

$$
B_i = \frac{-\frac{\partial c}{\partial \rho_i}}{\lambda \frac{\partial V}{\partial \rho_i}}
$$

in which λ is a Lagrangian multiplier that can be found by a bi-sectioning algorithm; m is a positive move-limit; η is a numerical damping coefficient. The introduction m and η is to ensure the stability of the iteration.

4.3 Sensitivity analysis

We refer to the sensitivity analysis in FEM, using the adjoint method to calculate the sensitivity of the objective function.

Rewrite the objective function by adding the zero function

$$c = \mathbf{F}^{\mathrm{T}}\mathbf{U} - \tilde{\mathbf{U}}^{\mathrm{T}}\left(\mathbf{K}\hat{\mathbf{U}} - \mathbf{F}\right) \tag{24}$$

where $\tilde{\mathbf{U}}$ is any arbitrary, but fixed real vector.

By the derivative of Equation (24) with respect to the design variable, we can obtain as

$$\frac{\partial c}{\partial \rho_i} = \mathbf{F}^{\mathrm{T}}\frac{\partial \mathbf{U}}{\partial \rho_i} - \tilde{\mathbf{U}}^{\mathrm{T}}\left(\frac{\partial \mathbf{K}}{\partial \rho_i}\hat{\mathbf{U}} + \mathbf{K}\frac{\partial \hat{\mathbf{U}}}{\partial \rho_i}\right) = \left(\mathbf{F}^{\mathrm{T}}\boldsymbol{\Phi} - \tilde{\mathbf{U}}^{\mathrm{T}}\mathbf{K}\right)\frac{\partial \hat{\mathbf{U}}}{\partial \rho_i} - \tilde{\mathbf{U}}^{\mathrm{T}}\frac{\partial \mathbf{K}}{\partial \rho_i}\hat{\mathbf{U}} \tag{25}$$

when $\tilde{\mathbf{U}}$ satisfies the adjoint equation $\mathbf{F}^{\mathrm{T}}\boldsymbol{\Phi} - \tilde{\mathbf{U}}^{\mathrm{T}}\mathbf{K} = 0$, we obtain directly that $\tilde{\mathbf{U}}^{\mathrm{T}} = \mathbf{F}^{\mathrm{T}}\boldsymbol{\Phi}\mathbf{K}^{-1}$, Equation (25) can be re-written as

$$\frac{\partial c}{\partial \rho_i} = -\mathbf{F}^{\mathrm{T}}\boldsymbol{\Phi}\mathbf{K}^{-1}\frac{\partial \mathbf{K}}{\partial \rho_i}\hat{\mathbf{U}} \tag{26}$$

In this way the sensitivity analysis of the objective function transforms to calculate the sensitivity of the stiffness matrix with respect to the design variable.

The sensitivity of the volume constraint with respect to the design variable is obtained as follows

$$\frac{\partial V}{\partial \rho_i} = \int_{\Omega} \phi_i \mathrm{d}\Omega \tag{27}$$

5   Numerical examples

In this section, numerical examples will be given to demonstrate the feasibility and efficiency of the proposed approach.

5.1 A square cantilever beam with a concentrated force applied on the middle of the free end

A square cantilever beam fixed on the left side and loaded with a concentrated force F at the middle of the right side, as shown in Fig.1(a), is now discussed. The problem domain is represented by 441 field nodes. The initial material distribution of the beam is shown in Fig.1(b), in which the black regions represent material while the white regions represent voids. The elastic material properties are chosen as Young's modulus $E = 3 \times 10^8 \mathrm{Pa}$, Possion's ratio $\mu = 0.3$, and the volume constraint is 40%.

(a) Cantilever beam problem   (b) Initial material distribution of the beam
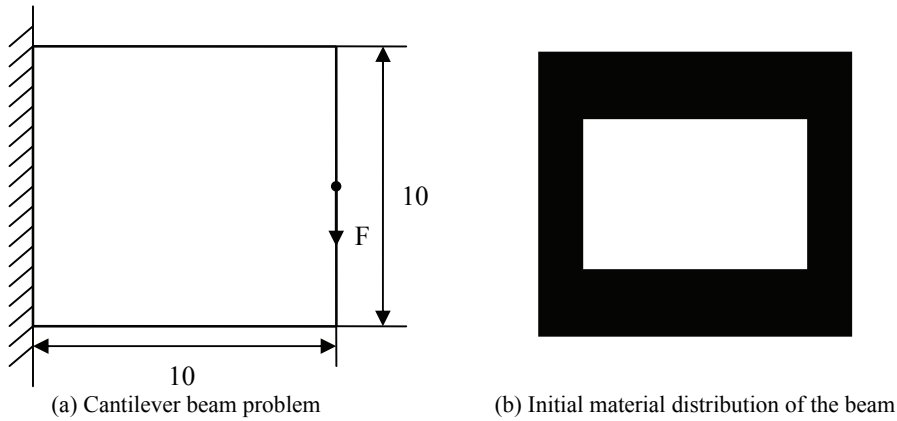
Figure 1

Fig.2 gives the optimization sequence of this example from the initial to the final steps of optimization. For the purpose of comparison, the optimization result obtained by FEM is shown in Fig.3(a) and the optimization result obtained by FEM with sensitivity filtering is shown in Fig.3(b). From these optimization results, it can be seen that the present approach can effectively eliminate the checkerboard phenomenon arising in FEM.

5.2 A cantilever beam with a concentrated force applied at the right lower corner

A cantilever beam is fixed on the left side and is loaded with a concentrated force F at the right lower corner, as shown in Fig.4(a). The problem domain is represented by 441 field nodes. As in the previous example, the elastic material properties are chosen as Young's modulus $E = 3 \times 10^8$ Pa, Possion's ratio $\mu = 0.3$, and the volume constraint is 50%.

The optimization result of beam obtained by the present method is shown in Fig.4(b). For comparison, the optimization result obtained by the FEM method is shown in Fig.4(c), and the optimization result obtained by RPIM with the relative density of the Gauss quadrature points as design variables is shown in Fig.4(d). From these optimization results, it can be seen that the present approach can effectively eliminate the checkerboard phenomenon arising in FEM and the checkerboard pattern with point state arising in the RPIM.
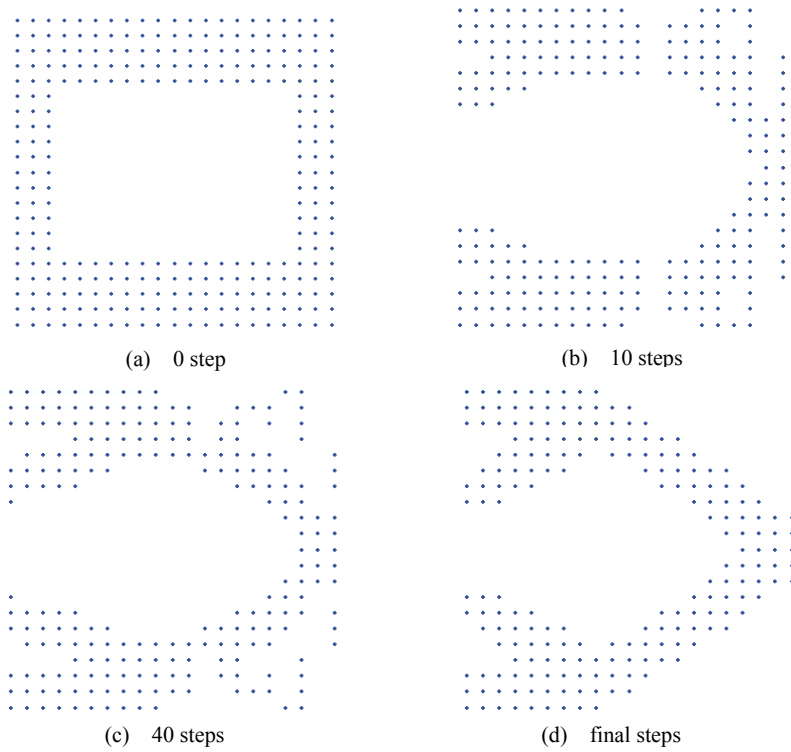
(a) 0 step

(b) 10 steps

(c) 40 steps

(d) final steps

Figure 2: Optimization sequence of example 1

(a) Optimization result by FEM

(b) Optimization result by FEM with sensitivity filtering

Figure 3

(a)   Cantilever beam problem

(b) Optimization result by present method
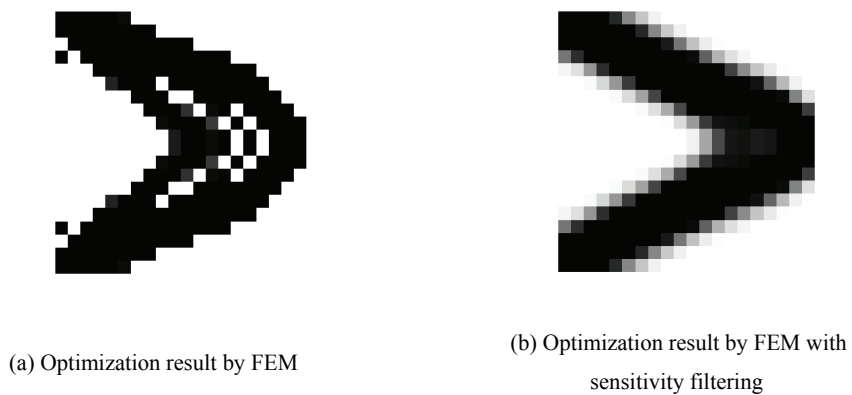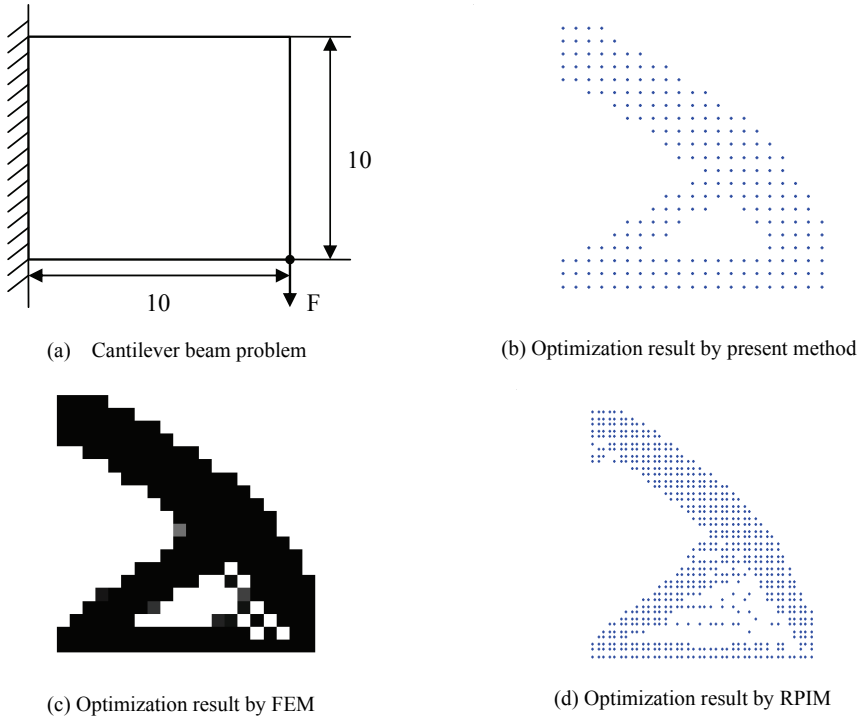
(c) Optimization result by FEM

(d) Optimization result by RPIM

Figure 4

6   Conclusions

In this paper, the topology optimization design is formulated using the FVMLPG method for two-dimensional elastostatics problems.

In FVMLPG, the finite volume method is combined with the meshless local Petrov-Galekin method. Both strains as well as displacements are interpolated, at randomly distributed points in a local domain, using the MLS approximation. Because choosing the strains as independent variables, the differentiation of the shape function is completely eliminated. And a direct interpolation method is used to impose the essential boundary conditions. This treatment of the essential boundary conditions is straightforward and very effective. It also significantly simplifies the procedure of imposing essential boundary conditions, and the essential boundary conditions are satisfied exactly.

Considering the relative density of the nodes as design variable and minimizing compliance as objective function, the mathematical formulation of the topology optimization is developed using the SIMP interpolation scheme. The adjoint sen-

sitivity analysis method is employed to formulate the sensitivities of the objective function and the volume constrain.

Several numerical examples are solved successfully by the proposed method. Numerical examples demonstrate that the proposed method is feasible and effective to deal with the topology optimization problems.

References

Atluri S.N.; Zhu T. (1998): A new meshless local Petrov-Galerkin (MLPG) approach in computational mechanics. *Computational Mechanics*, Vol.22, 117-127.

Atluri S.N.; Shen S. (2002): The Meshless Local Petrov-Galerkin (MLPG) Method: A Simple & Less-costly Alternative to the Finite Element and Boundary Element Methods. *CMES: Computer Modeling in Engineering & Science*, Vol.3, 11-51.

Atluri S.N.; Han Z.D.; Rajendran A.M. (2004): A New Implementation of the Meshless Finite Volume Method, Through the MLPG "Mixed" Approach. *CMES: Computer Modeling in Engineering & Sciences*, Vol.6, No.6, 491-514.

Belytschko T.; Lu Y.; Gu L. (1994): Element-free Galerkin method. *International Journal for Numerical Methods in Engineering*, 37: 229-256.

Bendsoe M.P.; Kikuchi N. (1988): Generating optimal topology in structural design using a homogenization method. *Computer Methods in Applied Mechanics and Engineering*, 71: 197-224.

Bendsoe M.P.; Sigmund O. (1999): Material interpolation schemes in topology optimization. *Archive of Applied Mechanics,* 69: 635-654.

Bendsoe M.P.; Sigmund O. (2003): *Topology Optimization: Theory, Methods, and Applications.* Berlin, Heidelberg, New York: Springer.

Cisilino A.P. (2006): Topology optimization of 2D potential problems using boundary elements. *CMES: Computer Modeling in Engineering & Sciences*, Vol.15, No.2, 99-106.

Chen S.S.; Liu Y.H.; Cen Z.Z. (2008): A combined approach of the MLPG method and nonlinear programming for lower-bound limit analysis. *CMES: Computer Modeling in Engineering & Sciences*, Vol.28, No.1, 39-56.

Fujii D.; Kikuchi N. (2000): Improvement of numerical instabilities in topology optimization using SLP method. *Structural and Multidisciplinary Optimization*,

19: 113-121.

Han Z.D.; Rajendran A.M.; Atluri S.N. (2005): Meshless local Petrov-Galerkin (MLPG) approaches for solving nonlinear problems with large deformations and rotations. *CMES: Computer Modeling in Engineering & Sciences*, Vol.10, No.1, 1-12.

Li S.; Atluri S.N. (2008a): Topology optimization of structures based on the MLPG mixed collocation method. *CMES: Computer Modeling in Engineering & Sciences*, Vol.26, No.1, 61-74.

Li S.; Atluri S.N. (2008b): The MLPG Mixed Collocation Method for Material Orientation and Topology Optimization of Anisotropic Solids and Structures. *CMES: Computer Modeling in Engineering & Sciences*, Vol.30, No.1, 37-56.

Michael Y.W.; Wang X.M. (2004): PDE-Driven Level Sets, Shape Sensitivity and Curvature Flow for Structural Topology Optimization. *CMES: Computer Modeling in Engineering & Sciences*, Vol.6, No.4, 373-396.

Michael Y.W.; Zhou S.W. (2004): Phase Field: A Variational Method for Structural Topology Optimization. *CMES: Computer Modeling in Engineering & Sciences*, Vol.6, No.6, 547-566.

Monaghan J.J. (1992): Smoothed particle hydrodynamics. *Annual Review of Astronomy and Astrophysics*, 30: 543-574.

Stolpe M.; Svanberg K. (2001): An alternative interpolation scheme for minimum compliance topology optimization. *Structural and Multidiscipline Optimization*, 22, 116-124.

Svanberg K. (1987): The method of moving asymptotes: a new method for structural optimization. *International Journal for Numerical Methods in Engineering*, 24: 359-373.

Tapp C.; Hansel W.; Mittelstedt C.; Becker W. (2004): Weight-Minimization of Sandwich Structures by a Heuristic Topology Optimization Algorithm. *CMES: Computer Modeling in Engineering & Sciences*, Vol.5, No.6, 563- 574.

Wang S.Y.; Lim K.M.; Khoo B.C.; Wang M.Y. (2007a): A geometric deformation constrained level set method for structural shape and topology optimization. *CMES: Computer Modeling in Engineering & Sciences*, Vol.18, No.3, 155-181.

Wang S.Y.; Lim K.M.; Khoo B.C.; Wang M.Y. (2007b): An unconditionally time-stable level set method and its application to shape and topology optimization. *CMES: Computer Modeling in Engineering & Sciences*, Vol.21, No.1, 1-40.

Wang S.Y.; Lim K.M.; Khoo B.C.; Wang M.Y. (2007c): On hole nucleation in topology optimization using the level set methods. *CMES: Computer Modeling in Engineering & Sciences*, Vol.21, No.3, 219-237.

Wang S.Y.; Lim K.M.; Khoo B.C.; Wang M.Y. (2008): A Hybrid Sensitivity Filtering Method for Topology Optimization. *CMES: Computer Modeling in Engineering & Sciences*, Vol.24, No.1, 21-50.

Wang S.Y.; Wang M.Y. (2006): Structural shape and topology optimization using an implicit free boundary parameterization method. *CMES: Computer Modeling in Engineering & Sciences*, Vol.13, No.2, 119-147.

Zheng J.; Long S.Y.; Xiong Y.B.; and Li G.Y. (2008): A topology optimization design for the continuum structure based on the meshless numerical technique. *CMES: Computer Modeling in Engineering & Sciences*, Vol.34, No.2, 137-154.

Zhou M.; Rozvany G.I.N. (1991): The COC algorithm Part II: topological, geometry and generalized shape optimization. *Computational Methods in Applied Mechanics and Engineering*, 89: 197-224.

Zhou M.; Rozvany G.I.N. (2001): On the validity of ESO type methods in topology optimization. *Structural and Multidiscipline Optimization*, 21, 80-83.

Zhou S.; Wang M.Y. (2006): 3D multi-material structural topology optimization with the generalized Cahn-Hilliard equations. *CMES: Computer Modeling in Engineering & Sciences*, Vol.16, No.2, 83-101.